XI International Conference on Computational Plasticity. Fundamentals and Applications
COMPLAS XI
E. Oñate, D.R.J. Owen, D. Peric and B. Suárez (Eds)

DISCONTINUOUS FAILURE IN A GRADIENT-ENHANCED CONTINUOUS DAMAGE MODEL: A REGULARISED DISPLACEMENT FRAMEWORK

ELENA TAMAYO-MAS, ANTONIO RODRÍGUEZ-FERRAN

Laboratori de Càlcul Numèric (LaCàN)
Departament de Matemàtica Aplicada III
Universitat Politècnica de Catalunya (UPC)
Campus Nord UPC, 08034, Barcelona, Spain
e-mail: {elena.tamayo, antonio.rodriguez-ferran}@upc.edu

Key words: Gradient damage model, Cohesive cracks, Smoothed displacements, Energy balance

Abstract. To simulate numerically a failure process, a new kind of model which combines the two traditional approaches (damage and fracture mechanics) has been proposed in the literature. The basic idea of these hybrid strategies is to employ regularised continuous models to describe the first stages of failure and discontinuous models to deal with the possible development of cracks.

Here, a new combined approach is presented. In order to describe damage inception and its diffuse propagation, an implicit gradient-enhanced continuum model based on smoothed displacements is used, where two different displacement fields coexist: (a) the standard displacements $\boldsymbol{u}$ and (b) the gradient-enriched displacement field $\widetilde{\boldsymbol{u}}$, which is the solution of a partial differential equation with $\boldsymbol{u}$ as the source term. Once the damage parameter exceeds a critical value, the continuous model is coupled to a discontinuous one. The eXtended Finite Element Method (X-FEM) is used to describe the growing cracks, whose direction of propagation is prescribed by the steepest descent direction of the damage profile and whose cohesive law is defined according to an energy balance. Therefore, the energy not yet dissipated by the continuous bulk is transmitted to the cohesive interface thus ensuring that the energy dissipated by the structure remains constant through the transition.

1 INTRODUCTION

To simulate numerically failure of quasi-brittle materials, two different kinds of approaches have usually been employed: (a) damage mechanics, which belongs to the family of continuous models and (b) fracture mechanics, which belongs to discontinuous models.

On the one hand, if damage mechanics analyses are carried out, the first stages of a failure process can be described. But these continuous models, which are characterised by a strain softening phenomenon, do not correctly reflect the energy dissipated in the fracture process zone [1]. Numerically, if stress-strain laws with softening are used, physically unrealistic results are obtained. To overcome this limitation, regularisation techniques may be employed to introduce non-locality into the model, either by integral-type [2, 3] or gradient-type [4, 5] approaches. However, if continuum models are used to describe the final stage of failure, numerical interaction between the physically separated parts of the body remains thus obtaining unrealistic results.

On the other hand, by means of fracture mechanics analyses, the last stages of failure may be described. These discontinuous models, which are based on the cohesive zone concept [6], can deal with evolving cracks and material separation but do not allow to describe neither damage inception nor its diffuse propagation [7].

In order to achieve a better description of the entire failure process, a new kind of model which combines these two traditional strategies has emerged [8–12]. The basic idea of these hybrid strategies is to use damage mechanics in order to characterise strain localisation and the accumulation of damage and fracture mechanics in order to deal with the possible formation of evolving macrocracks.

In this work, a new contribution in this direction is presented, see Figure 1. A gradient-enhanced damage model based on smoothed displacements [13] is used for the continuum. When the damage parameter exceeds a critical threshold D_{crit}, this regularised continuum model is coupled to a discontinuous one: a propagating crack, which is modelled by means of the X-FEM [14, 15], replaces the damaged zone and avoids formation of spurious damage growth. The discontinuity is completely characterised by the regularised continuum. On the one hand, the crack evolves according to the direction dictated by the steepest descent direction of the already formed damage profile. On the other hand, its cohesive law is defined by means of an energy balance in such a way that the energy which would be dissipated by the continuum is transferred to the crack.

An outline of this paper follows. The new continuous-discontinuous methodology is formulated in Section 2. In Section 3, the energy criterion used to define the cohesive crack is presented. To validate the proposed methodology, a three-point bending test is carried out in Section 4. In order to restrict attention to the proposed energy balance, a local continuum bulk is considered in Section 4.1. In Section 4.2, the same benchmark test is carried out with a non-local continuum bulk. The concluding remarks of Section 5 close this paper.

2 MODEL FORMULATION

2.1 Discontinuous displacements

Consider the domain Ω bounded by $\Gamma = \Gamma_u \cup \Gamma_t \cup \Gamma_d$, as shown in Figure 2. Prescribed displacements are imposed on Γ_u, prescribed tractions are imposed on Γ_t and the boundary

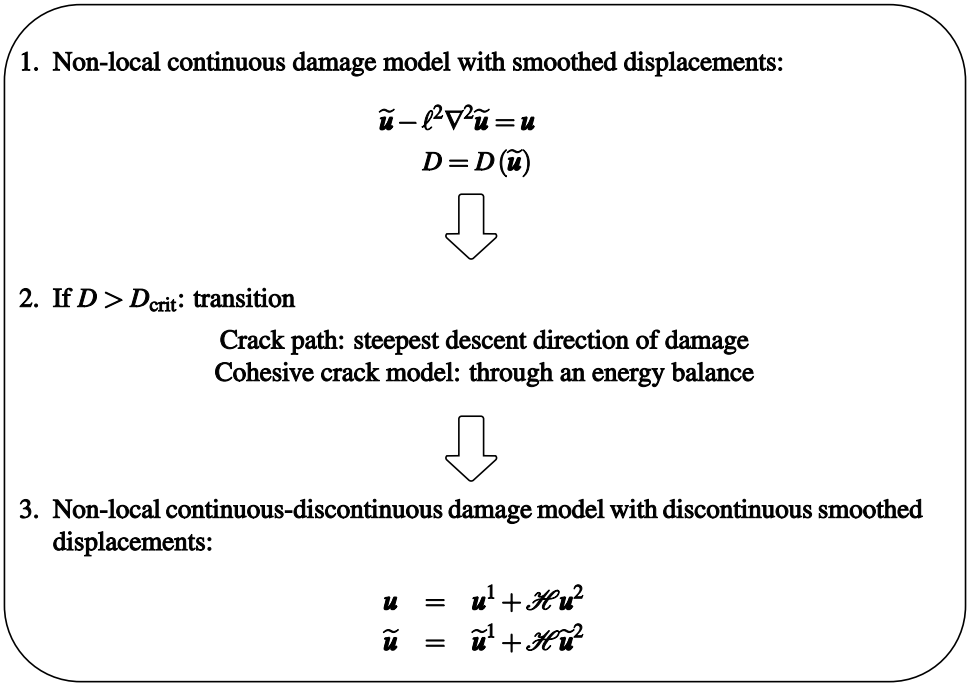

Figure 1: Proposed continuous-discontinuous strategy.

Γ_d consists of the boundary of the crack.

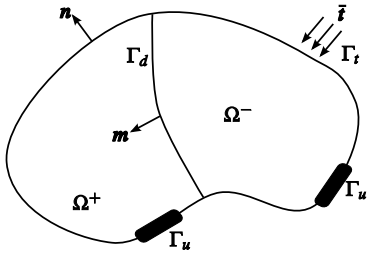

Figure 2: Notations for a body with a crack subjected to loads and imposed displacements.

By means of the X-FEM, the displacement field $\boldsymbol{u}$ can be decomposed as

$$\boldsymbol{u}(\boldsymbol{x}) = \boldsymbol{u}^1(\boldsymbol{x}) + \mathcal{H}(\boldsymbol{x})\,\boldsymbol{u}^2(\boldsymbol{x}) \qquad \text{in } \bar{\Omega} = \Omega \cup \Gamma \tag{1}$$

where $\boldsymbol{u}^i(\boldsymbol{x})$ $(i = 1, 2)$ are continuous fields and

$$\mathcal{H}(\boldsymbol{x}) = \begin{cases} 1 & \text{if} \quad \boldsymbol{x} \in \bar{\Omega}^+ \\ -1 & \text{if} \quad \boldsymbol{x} \in \bar{\Omega}^- \end{cases} \tag{2}$$

is the Heaviside function centred at Γ_d. The continuous part $\boldsymbol{u}^1(\boldsymbol{x})$ corresponds to the displacement field without any crack, while is the discontinuous displacement $\mathcal{H}(\boldsymbol{x})\,\boldsymbol{u}^2(\boldsymbol{x})$ the additional field that models the crack.

A similar decomposition holds for the smoothed displacements $\widetilde{\boldsymbol{u}}$

$$\widetilde{\boldsymbol{u}}\left(\boldsymbol{x}\right)=\widetilde{\boldsymbol{u}}^{1}\left(\boldsymbol{x}\right)+\mathcal{H}\left(\boldsymbol{x}\right)\widetilde{\boldsymbol{u}}^{2}\left(\boldsymbol{x}\right) \tag{3}$$

where $\widetilde{\boldsymbol{u}}^{i}\left(\boldsymbol{x}\right)$ $(i=1,2)$ are continuous fields.

2.2 Governing equations

The strong form of the equilibrium equation and boundary conditions for the body $\bar{\Omega}$ without body forces is given by

$$\begin{aligned}
\nabla\cdot\boldsymbol{\sigma} &= \mathbf{0} \quad \text{in } \Omega && \text{(4a)}\\
\boldsymbol{\sigma}\cdot\boldsymbol{n} &= \bar{\boldsymbol{t}} \quad \text{on } \Gamma_t && \text{(4b)}\\
\boldsymbol{\sigma}\cdot\boldsymbol{m} &= \bar{\boldsymbol{t}}_d \quad \text{on } \Gamma_d && \text{(4c)}\\
\boldsymbol{u} &= \boldsymbol{u}^{*} \quad \text{on } \Gamma_u && \text{(4d)}
\end{aligned}$$

where $\boldsymbol{\sigma}$ is the Cauchy stress tensor, $\boldsymbol{u}^{*}$ is a prescribed displacement, $\bar{\boldsymbol{t}}$ is the load on the boundary and $\bar{\boldsymbol{t}}_d$ is the load on the discontinuity surface. Note that $\boldsymbol{n}$ is the outward unit normal to the body and $\boldsymbol{m}$ is the inward unit normal to Ω^{+} on Γ_d, see Figure 2.

For convenience, and to complete the strong form of the mechanical problem, only an isotropic damage model

$$\boldsymbol{\sigma}\left(\boldsymbol{x}\right)=\left[1-D\left(\boldsymbol{x}\right)\right]\boldsymbol{C}:\boldsymbol{\varepsilon}\left(\boldsymbol{x}\right) \tag{5}$$

is considered, where $\boldsymbol{\varepsilon}\left(\boldsymbol{x}\right)=\nabla^{s}\boldsymbol{u}\left(\boldsymbol{x}\right)$ is the small strain tensor, $\boldsymbol{C}$ is the fourth-order tensor of elastic moduli and D is the isotropic damage parameter ($0\leq D\leq 1$ and $\dot{D}\geq 0$). Nevertheless, the gradient formulation based on smoothed displacements may be extended to other models such as plasticity [16].

In order to regularise the problem, the second-order diffusion partial differential equation

$$\widetilde{\boldsymbol{u}}-\ell^{2}\nabla^{2}\widetilde{\boldsymbol{u}}\left(\boldsymbol{x}\right)=\boldsymbol{u}\left(\boldsymbol{x}\right)\qquad \text{in}\,\Omega\setminus\Gamma_d \tag{6}$$

is coupled with the mechanical equations. Both for the standard and the enhanced displacement fields, combined boundary conditions

$$\left.\begin{aligned}
\widetilde{\boldsymbol{u}}^{i}\cdot\boldsymbol{n} &= \boldsymbol{u}^{i}\cdot\boldsymbol{n}\\
\nabla\left(\widetilde{\boldsymbol{u}}^{i}\cdot\boldsymbol{t}\right)\cdot\boldsymbol{n} &= \nabla\left(\boldsymbol{u}^{i}\cdot\boldsymbol{t}\right)\cdot\boldsymbol{n}
\end{aligned}\right\}\ \text{on }\Gamma
\qquad
\left.\begin{aligned}
\widetilde{\boldsymbol{u}}^{i}\cdot\boldsymbol{m} &= \boldsymbol{u}^{i}\cdot\boldsymbol{m}\\
\nabla\left(\widetilde{\boldsymbol{u}}^{i}\cdot\boldsymbol{t}\right)\cdot\boldsymbol{m} &= \nabla\left(\boldsymbol{u}^{i}\cdot\boldsymbol{t}\right)\cdot\boldsymbol{m}
\end{aligned}\right\}\ \text{on }\Gamma_d \tag{7}$$

where $i=1,2$, are proposed: Dirichlet boundary conditions are prescribed for the normal component of the displacement field whereas non-homogeneous Neumann boundary conditions are imposed for the tangential one. These combined conditions satisfy the necessary properties for regularisation: (a) reproducibility of order 1 ($\boldsymbol{u}=\widetilde{\boldsymbol{u}}$ if $\boldsymbol{u}$ is a linear field), (b) displacement smoothing along the boundary and (c) volume preservation [17].

2.3 Variational formulation

The space of trial standard displacements is characterised by the function defined in Eq. (1), where

$$\boldsymbol{u}^1, \boldsymbol{u}^2 \in \mathcal{U}_{\boldsymbol{u}} = \left\{ \boldsymbol{u} \mid \boldsymbol{u} \in H^1(\Omega) \text{ and } \boldsymbol{u}_{|\Gamma_u} = \boldsymbol{u}^* \right\} \tag{8}$$

with $H^1(\Omega)$ a Sobolev space. Analogously, the space of admissible displacement variations is defined by the weight function $\boldsymbol{\omega}(\boldsymbol{x}) = \boldsymbol{\omega}^1(\boldsymbol{x}) + \mathcal{H}(\boldsymbol{x})\boldsymbol{\omega}^2(\boldsymbol{x})$ with

$$\boldsymbol{\omega}^1, \boldsymbol{\omega}^2 \in \mathcal{W}_{\boldsymbol{u},\boldsymbol{0}} = \left\{ \boldsymbol{\omega} \mid \boldsymbol{\omega} \in H^1(\Omega) \text{ and } \boldsymbol{\omega}_{|\Gamma_u} = \boldsymbol{0} \right\} \tag{9}$$

Following standard procedures, the equilibrium equation (4a) can be cast in a variational form, thus leading to

$$\int_\Omega \nabla^s \boldsymbol{\omega}^1 : \boldsymbol{\sigma} \, \mathrm{d}\Omega = \int_{\Gamma_t} \boldsymbol{\omega}^1 \cdot \bar{\boldsymbol{t}} \, \mathrm{d}\Gamma \qquad \forall \boldsymbol{\omega}^1 \in H^1(\Omega) \tag{10a}$$

$$\int_\Omega \mathcal{H} \nabla^s \boldsymbol{\omega}^2 : \boldsymbol{\sigma} \, \mathrm{d}\Omega + 2 \int_{\Gamma_d} \boldsymbol{\omega}^2 \cdot \bar{\boldsymbol{t}}_d \, \mathrm{d}\Gamma = \int_{\Gamma_t} \mathcal{H} \boldsymbol{\omega}^2 \cdot \bar{\boldsymbol{t}} \, \mathrm{d}\Gamma \qquad \forall \boldsymbol{\omega}^2 \in H^1(\Omega) \tag{10b}$$

where at the discontinuity Γ_d,

$$\dot{\bar{\boldsymbol{t}}}_d = f\left([\![\dot{\boldsymbol{u}}]\!] \right) \tag{11}$$

with f relating traction rate $\dot{\bar{\boldsymbol{t}}}_d$ and displacement jump rate $[\![\dot{\boldsymbol{u}}]\!]$.

Similarly to the equilibrium equation, the regularisation PDE (6) is also cast in a weak form. Characterising the space of trial smoothed displacements $\widetilde{\boldsymbol{u}}$ by the function defined in Eq. (3), with $\boldsymbol{u}^1, \boldsymbol{u}^2 \in \mathcal{U}_{\boldsymbol{u}}$, one obtains

$$\begin{aligned}
\int_\Omega \boldsymbol{\omega}^1 \cdot (\widetilde{\boldsymbol{u}}^1 + \mathcal{H}\widetilde{\boldsymbol{u}}^2) \, \mathrm{d}\Omega \;+\; & \ell^2 \int_\Omega \nabla \boldsymbol{\omega}^1 : \left(\nabla \widetilde{\boldsymbol{u}}^1 + \mathcal{H} \nabla \widetilde{\boldsymbol{u}}^2 \right) \mathrm{d}\Omega + 2\ell^2 \int_{\Gamma_d} \omega_t^1 \left(\nabla \left(\boldsymbol{u}^2 \cdot \boldsymbol{t} \right) \cdot \boldsymbol{m} \right) \mathrm{d}\Gamma = \\
= \; & \int_\Omega \boldsymbol{\omega}^1 \cdot (\boldsymbol{u}^1 + \mathcal{H}\boldsymbol{u}^2) \, \mathrm{d}\Omega + \ell^2 \int_{\Gamma \setminus \Gamma_d} \omega_t^1 \left(\nabla \left(\boldsymbol{u}^1 \cdot \boldsymbol{t} \right) \cdot \boldsymbol{n} + \mathcal{H} \nabla \left(\boldsymbol{u}^2 \cdot \boldsymbol{t} \right) \cdot \boldsymbol{n} \right) \mathrm{d}\Gamma
\end{aligned} \tag{12a}$$

$$\begin{aligned}
\int_\Omega \boldsymbol{\omega}^2 \cdot (\mathcal{H}\widetilde{\boldsymbol{u}}^1 + \widetilde{\boldsymbol{u}}^2) \, \mathrm{d}\Omega \;+\; & \ell^2 \int_\Omega \nabla \boldsymbol{\omega}^2 : \left(\mathcal{H} \nabla \widetilde{\boldsymbol{u}}^1 + \nabla \widetilde{\boldsymbol{u}}^2 \right) \mathrm{d}\Omega + 2\ell^2 \int_{\Gamma_d} \omega_t^2 \left(\nabla \left(\boldsymbol{u}^1 \cdot \boldsymbol{t} \right) \cdot \boldsymbol{m} \right) \mathrm{d}\Gamma = \\
= \; & \int_\Omega \boldsymbol{\omega}^2 \cdot (\mathcal{H}\boldsymbol{u}^1 + \boldsymbol{u}^2) \, \mathrm{d}\Omega + \ell^2 \int_{\Gamma \setminus \Gamma_d} \omega_t^2 \left(\mathcal{H} \nabla \left(\boldsymbol{u}^1 \cdot \boldsymbol{t} \right) \cdot \boldsymbol{n} + \nabla \left(\boldsymbol{u}^2 \cdot \boldsymbol{t} \right) \cdot \boldsymbol{n} \right) \mathrm{d}\Gamma
\end{aligned} \tag{12b}$$

$\forall \boldsymbol{\omega}^1, \boldsymbol{\omega}^2 \in \mathcal{W}_{\boldsymbol{u},\boldsymbol{0}}$, where $\boldsymbol{t}$ is the unit tangent to the boundary.

2.4 Finite element discretisation

In combined strategies, the transition between the continuous and the discontinuous approach takes place when a critical situation is achieved. In a damaging continuum approach, for example, this critical situation occurs when the damage parameter at one integration point exceeds a critical damage value set *a priori*. Employing an extended

finite element strategy to prevent remeshing and other kinds of techniques, Eq. (1) and (3) read, in the domain of an element with enhanced nodes,

$$\mathbf{u}(\boldsymbol{x}) = \mathbf{N}(\boldsymbol{x})\mathbf{u}^1 + \mathcal{H}(\boldsymbol{x})\mathbf{N}(\boldsymbol{x})\mathbf{u}^2 \tag{13a}$$

$$\widetilde{\mathbf{u}}(\boldsymbol{x}) = \mathbf{N}(\boldsymbol{x})\widetilde{\mathbf{u}}^1 + \mathcal{H}(\boldsymbol{x})\mathbf{N}(\boldsymbol{x})\widetilde{\mathbf{u}}^2 \tag{13b}$$

where $\mathbf{N}$ is the matrix of standard finite element shape functions, $\mathbf{u}^1$, $\widetilde{\mathbf{u}}^1$ are the basic nodal degrees of freedom and $\mathbf{u}^2$, $\widetilde{\mathbf{u}}^2$ are the enhanced ones. The discrete format of the problem fields leads to the four discrete weak governing equations

$$\int_\Omega \mathbf{B}^T\boldsymbol{\sigma}\,\mathrm{d}\Omega = \int_{\Gamma_t} \mathbf{N}^T\bar{\boldsymbol{t}}\,\mathrm{d}\Gamma \tag{14a}$$

$$\int_\Omega \mathcal{H}\mathbf{B}^T\boldsymbol{\sigma}\,\mathrm{d}\Omega + 2\int_{\Gamma_d} \mathbf{N}^T\bar{\boldsymbol{t}}_d\,\mathrm{d}\Gamma = \int_{\Gamma_t} \mathcal{H}\mathbf{N}^T\bar{\boldsymbol{t}}\,\mathrm{d}\Gamma \tag{14b}$$

$$(\mathbf{M}+\ell^2\mathbf{D})\widetilde{\mathbf{u}}^1 + (\mathbf{M}_\mathcal{H}+\ell^2\mathbf{D}_\mathcal{H})\widetilde{\mathbf{u}}^2 = (\mathbf{M}+\ell^2\boldsymbol{C}^{\Gamma\setminus\Gamma_d,\boldsymbol{n}})\mathbf{u}^1 + (\mathbf{M}_\mathcal{H}+\ell^2(\boldsymbol{C}_\mathcal{H}^{\Gamma\setminus\Gamma_d,\boldsymbol{n}} - 2\boldsymbol{C}^{\Gamma_d,\boldsymbol{m}}))\mathbf{u}^2 \tag{14c}$$

$$(\mathbf{M}_\mathcal{H}+\ell^2\mathbf{D}_\mathcal{H})\widetilde{\mathbf{u}}^1 + (\mathbf{M}+\ell^2\mathbf{D})\widetilde{\mathbf{u}}^2 = (\mathbf{M}_\mathcal{H}+\ell^2(\boldsymbol{C}_\mathcal{H}^{\Gamma\setminus\Gamma_d,\boldsymbol{n}} - 2\boldsymbol{C}^{\Gamma_d,\boldsymbol{m}}))\mathbf{u}^1 + (\mathbf{M}+\ell^2\boldsymbol{C}^{\Gamma\setminus\Gamma_d,\boldsymbol{n}})\mathbf{u}^2 \tag{14d}$$

where $\mathbf{B}$ is the matrix of shape function derivatives and

$$\mathbf{M} = \int_\Omega \mathbf{N}^T\mathbf{N}\,\mathrm{d}\Omega \qquad \mathbf{D} = \int_\Omega \nabla\mathbf{N}^T\nabla\mathbf{N}\,\mathrm{d}\Omega \tag{15a}$$

$$\mathbf{M}_\mathcal{H} = \int_\Omega \mathcal{H}\mathbf{N}^T\mathbf{N}\,\mathrm{d}\Omega \qquad \mathbf{D}_\mathcal{H} = \int_\Omega \mathcal{H}\nabla\mathbf{N}^T\nabla\mathbf{N}\,\mathrm{d}\Omega \tag{15b}$$

$$\boldsymbol{C}^{\Gamma,\boldsymbol{n}} = \int_\Gamma \mathbf{N}^T\boldsymbol{t}\boldsymbol{t}^T\left[\frac{\partial\mathbf{N}}{\partial x}n_x + \frac{\partial\mathbf{N}}{\partial y}n_y\right]\mathrm{d}\Gamma \qquad \boldsymbol{C}_\mathcal{H}^{\Gamma,\boldsymbol{n}} = \int_\Gamma \mathcal{H}\mathbf{N}^T\boldsymbol{t}\boldsymbol{t}^T\left[\frac{\partial\mathbf{N}}{\partial x}n_x + \frac{\partial\mathbf{N}}{\partial y}n_y\right]\mathrm{d}\Gamma \tag{15c}$$

Some remarks about the discretisation:

- Eq. (14a) is the standard non-linear system of equilibrium equations, while Eq. (14b) deals with the contribution of the crack, which is multiplied by a factor of two due to the chosen definition of the Heaviside function, see Eq. (2).

- Matrices $\mathbf{M}$ and $\mathbf{D}$ are the constant mass and diffusivity matrices already obtained in [13]. The enriched matrices $\mathbf{M}_\mathcal{H}$ and $\mathbf{D}_\mathcal{H}$ are also constant, once the finite element is cracked.

- Matrices $\boldsymbol{C}^{\Gamma\setminus\Gamma_d,\boldsymbol{n}}$, $\boldsymbol{C}_\mathcal{H}^{\Gamma\setminus\Gamma_d,\boldsymbol{n}}$ and $\boldsymbol{C}^{\Gamma_d,\boldsymbol{m}}$ contain contributions from the combined boundary conditions (7). Since Dirichlet boundary conditions are prescribed for the normal component of the displacement field on Γ, the normal component of the weight function $\boldsymbol{\omega}$ vanishes on the boundary thus leading to

$$\int_\Gamma \boldsymbol{\omega}\nabla\widetilde{\boldsymbol{u}}\cdot\boldsymbol{n}\,\mathrm{d}\Gamma = \int_\Gamma \omega_t\nabla\left(\widetilde{\boldsymbol{u}}\cdot\boldsymbol{t}\right)\cdot\boldsymbol{n}\,\mathrm{d}\Gamma = \int_\Gamma \omega_t\nabla\left(\boldsymbol{u}\cdot\boldsymbol{t}\right)\cdot\boldsymbol{n}\,\mathrm{d}\Gamma \tag{16a}$$

  Again, $\boldsymbol{C}^{\Gamma_d,\boldsymbol{m}}$ is multiplied by a factor of two because of the Heaviside function.

- The symmetry of the resulting discretisation is due to the property $\mathcal{H}\mathcal{H} = +1$, which is derived from Eq. (2).

3 ENERGETICALLY EQUIVALENT CRACKS

In the proposed strategy, the transition between the continuous and the combined approach takes place when a critical situation is achieved, whose definition depends on the underlying continuous model. If a damage model is considered, the transition takes place when the damage value exceeds a critical threshold D_{crit}. Once this critical value is reached, a crack described by a cohesive law is initiated, damage value is fixed to D_{crit} and the bulk material unloads.

We propose to characterise the evolving crack by the regularised bulk. On the one hand, the direction of propagation must be determined. Although in a regularised continuous model, the crack growth cannot be analytically derived, the background can be used to deduce it. Here, the discontinuity is extended according to the steepest descent direction of the damage profile, thus avoiding the use of special tracking techniques. On the other hand, the cohesive law must be defined. The strategy here used is based on the idea that the energy which would be dissipated by a continuum approach is conserved if a combined strategy is used, see [8, 9].

Consider first the continuous approach and a damaged band λ_D. Then, in this zone of the structure, the dissipated energy can be expressed as

$$\Psi_C = \int_{\lambda_D} \psi_C \,\mathrm{d}\Omega = \int_{\lambda_D} \int_0^{t_f} \boldsymbol{\sigma}_C \cdot \dot{\boldsymbol{\varepsilon}}_C \,\mathrm{d}t \,\mathrm{d}\Omega \tag{17}$$

where the subscript C stands for *Continuous strategy* and $\dot{\boldsymbol{\varepsilon}}_C$ is the tensor of the strain rate.

Consider now the combined approach. In λ_D, the dissipated energy can be decomposed into two contributions

$$\Psi_{CD} = \Psi_{CD}^{\text{bulk}} + \Psi_{CD}^{\text{crack}} = \int_{\lambda_D} \int_0^{t_f} \boldsymbol{\sigma}_{CD} \cdot \dot{\boldsymbol{\varepsilon}}_{CD} \,\mathrm{d}t \,\mathrm{d}\Omega + \Psi_{CD}^{\text{crack}} \tag{18}$$

where the subscript CD stands for *Continuous-Discontinuous strategy*, Ψ_{CD}^{bulk} is the dissipated energy of the bulk and Ψ_{CD}^{crack} is the fracture energy.

Hence, imposing energy balance

$$\Psi_C = \Psi_{CD} \tag{19}$$

see Figure 3, the fracture energy

$$\Psi_{CD}^{\text{crack}} = \Psi_C - \Psi_{CD}^{\text{bulk}} \tag{20}$$

is computed and can be transferred to the crack at the moment of the transition.

In order to estimate the fracture energy, different techniques can be employed. In [9], an analytical estimation of Ψ_{CD}^{crack}, and thus, of the crack stiffness, is computed. Nevertheless, with this procedure, the fracture energy is overestimated. Indeed, by means of these

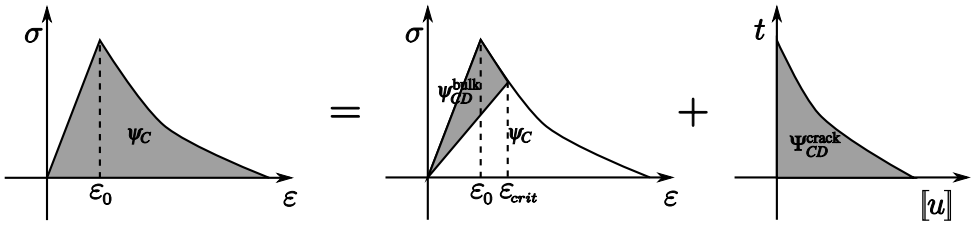

Figure 3: Energy balance.

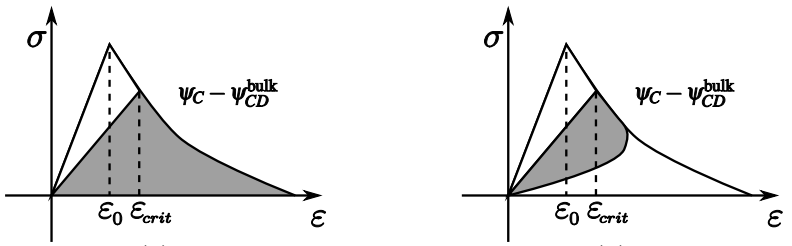

Figure 4: Energy not yet dissipated in the damage band which is transmitted to the cohesive crack and is dissipated by the continuous-discontinuous model, considering that by the continuous strategy, (a) all the points of λ_D download following the softening branch and (b) points of λ_D download following both softening and elastic branches.

assumptions, in all points across the damage band λ_D, the energy $\Psi_C - \Psi_{CD}^{\text{bulk}}$ depicted in Figure 4(a) is transferred to the crack. However, in some of these points, the continuous strategy would dissipate less energy, see Figure 4(b).

As suggested by this discussion, we propose to employ a new methodology which takes into account, for each point across the damage band λ_D, the unloading behaviour (both softening and secant) of the continuous bulk. Since the continuous unloading branch is only known up to the activation of the continuous-discontinuous strategy, we propose to approximate it by the tangent to the transition point. By means of this strategy, the dissipated energy Ψ_{CD}^{crack} is more accurately estimated, although it cannot be exactly computed. Again, as in [9], the accuracy of this strategy increases considerably if the crack is activated at a later stage of the failure process.

4 APPLICATION TO A THREE-POINT BENDING TEST

The new methodology is illustrated on a three-point bending test. In order to cause localisation, a weakened region is considered, see Figure 5. The test is carried out according to a simplified Mazars criterion and the trilinear softening law

$$D = \begin{cases} 0 & \text{if} \quad 0 \le Y \le Y_0 \\ \frac{Y_f}{Y_f - Y_0}\left(1 - \frac{Y_0}{Y}\right) & \text{if} \quad Y_0 \le Y \le Y_f \\ 1 & \text{if} \quad Y_f \le Y \end{cases} \tag{21}$$

Based on this damage evolution, the linear traction-separation law

$$\bar{\boldsymbol{t}}_d = \left\{ \begin{array}{c} \bar{t}_n \\ \bar{t}_s \end{array} \right\} = \mathbf{T} \left\{ \begin{array}{c} [\![\boldsymbol{u}]\!]_n \\ [\![\boldsymbol{u}]\!]_s \end{array} \right\} + \left\{ \begin{array}{c} t_{\text{crit}} \\ 0 \end{array} \right\} = \left(\begin{array}{cc} T_n & 0 \\ 0 & 0 \end{array} \right) \left\{ \begin{array}{c} [\![\boldsymbol{u}]\!]_n \\ [\![\boldsymbol{u}]\!]_s \end{array} \right\} + \left\{ \begin{array}{c} t_{\text{crit}} \\ 0 \end{array} \right\} \tag{22}$$

is prescribed, where imposing $\Psi_{CD}^{\text{crack}} = \int_0^\infty t_n \, \mathrm{d}[\![\boldsymbol{u}]\!]_n$, $T_n = -\frac{1}{2} \frac{t_{\text{crit}}^2}{\Psi_{CD}^{\text{crack}}}$.

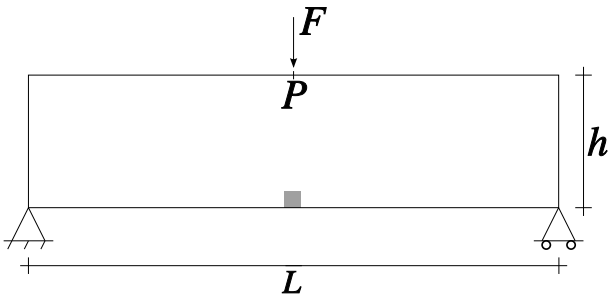

Figure 5: Three-point bending test: problem statement.

The geometric and material parameters for this test are summarised in Table 1.

Table 1: Three-point bending test: geometric and material parameters.

Meaning	Symbol	Value
Length of the specimen	L	3 mm
Width of the specimen	h	1 mm
Young's modulus	E	30 000 MPa
Idem of weaker part	E_W	27 000 MPa
Damage threshold	Y_0	10^{-4}
Final strain	Y_f	1.25×10^{-2}
Poisson's coefficient	ν	0.0
Critical damage	D_{crit}	0.995

4.1 Local bulk

First, and in order to focus on the proposed energy balance, a local continuum damage model is considered. The force-displacement curves and the damage profiles with the deformed meshes are shown in Figure 6. For comparison purposes, three kinds of results are shown. On the one hand, the continuous (C) results are plotted. On the other hand, two different continuous-discontinuous (CD) results are shown: the ones obtained with (a) the analytical estimation of the dissipated energy and (b) the proposed methodology, which does not overestimate the fracture energy. As seen, it increases the accuracy when estimating Ψ_{CD}^{crack}.

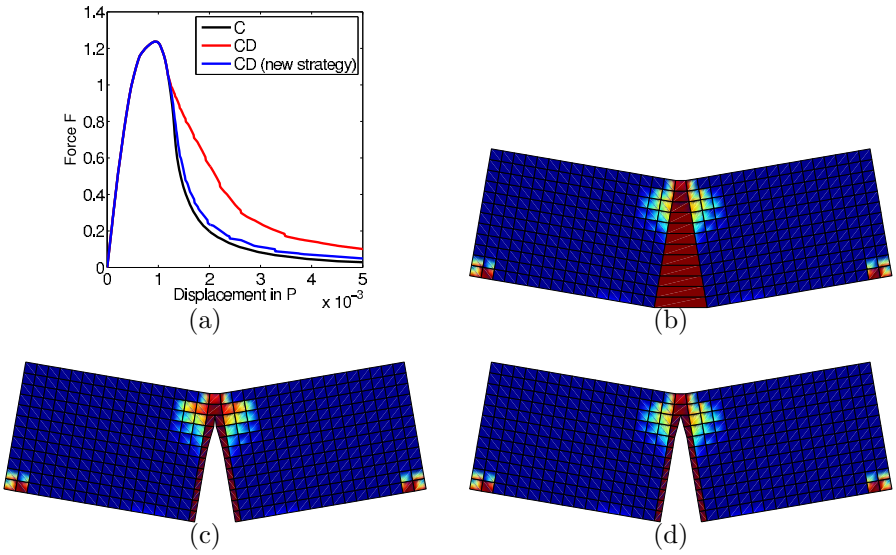

Figure 6: Three-point bending test with a local damage bulk: (a) force-displacement curves; final damage profiles with deformed meshes (×50) obtained with (b) the C strategy, (c) the CD strategy which overestimates the fracture energy and (d) the CD strategy based on the new proposed methodology.

4.2 Non-local bulk

As a second test, the same benchmark example is carried out with a non-local damage bulk. Results are shown in Figure 7. Again, three kinds of results are shown. As seen, the proposed methodology allows to estimate properly Ψ_{CD}^{crack} making the continuous and the continuous-discontinuous strategies energetically equivalent.

5 CONCLUSIONS

A new strategy to simulate an entire failure process is proposed: a gradient-enriched formulation based on smoothed displacements is enhanced with a discontinuous interpolation of the problem fields in order to describe its final stages, where macroscopic cracks can arise.
The main features of this new combined strategy are summarised here:

- The gradient-enhanced approach with smoothed displacements is able to obtain physically realistic results. Combined boundary conditions must be imposed on the boundary to solve the regularisation PDE.

- At the end of each time step, the strategy checks if the critical situation is achieved. If the transition criterion is satisfied, a discrete crack whose properties depend on the underlying continuous, is introduced.

  – This evolving crack propagates across the bulk according to the direction determined by the already damage profile.

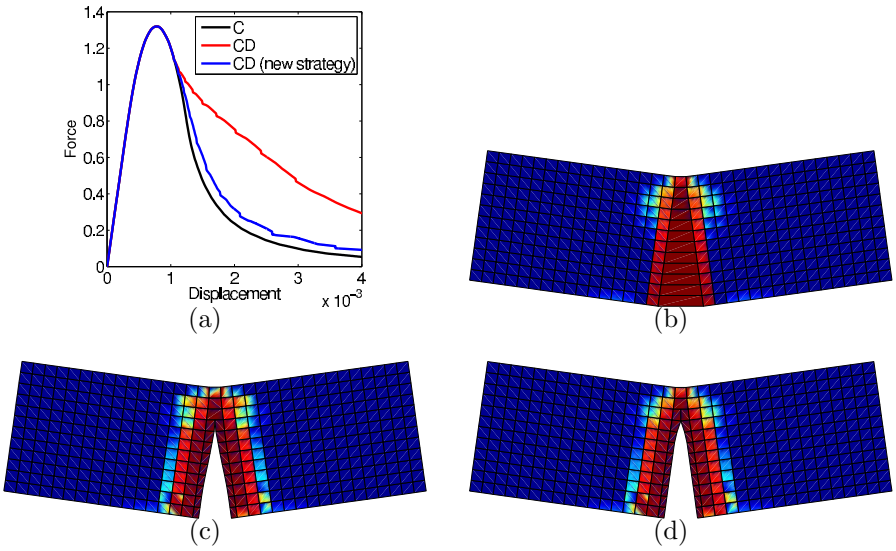

Figure 7: Three-point bending test with a non-local damage bulk: (a) force-displacement curves; final damage profiles with deformed meshes (×50) obtained with (b) the C strategy, (c) the CD strategy which overestimates the fracture energy and (d) the CD strategy based on the new proposed methodology.

  - The cohesive law is defined through an energy balance: the energy remaining to be dissipated by the continuum approach is transmitted to the cohesive zone.

- Once the crack is introduced, both standard displacements $\boldsymbol{u}$ and gradient-enhanced displacement field $\widetilde{\boldsymbol{u}}$ may admit discontinuities.

References

[1] M. Jirásek. Mathematical analysis of strain localization. *Revue Européenne de Génie Civil*, 11(7-8):977–991, 2007.

[2] Z. P. Bažant and M. Jirásek. Nonlocal integral formulations of plasticity and damage: survey of progress. *Journal of Engineering Mechanics*, 128(11):1119–1149, 2002.

[3] G. Pijaudier-Cabot and Z. P. Bažant. Nonlocal damage theory. *Journal of Engineering Mechanics - ASCE*, 118(10):1512–1533, 1987.

[4] R. de Borst, J. Pamin, R. H. J. Peerlings, and L. J. Sluys. On gradient-enhanced damage and plasticity models for failure in quasi-brittle and frictional materials. *Computational Mechanics*, 17(1-2):130–141, 1995.

[5] R. H. J. Peerlings, R. de Borst, W. A. M. Brekelmans, and M. G. D. Geers. Gradient-enhanced damage modelling of concrete fracture. *Mechanics of Cohesive-frictional Materials*, 3(4):323–342, 1998.

[6] A. Hillerborg, M. Modeer, and P. A. Petersson. Analysis of crack formation and crack growth in concrete by means of fracture mechanics and finite elements. *Cement and Concrete Research*, 6(6):773–782, 1976.

[7] J. Mazars and G. Pijaudier-Cabot. From damage to fracture mechanics and conversely: a combined approach. *International Journal of Solids and Structures*, 33(20-22):3327–3342, 1996.

[8] F. Cazes, M. Coret, A. Combescure, and A. Gravouil. A thermodynamic method for the construction of a cohesive law from a nonlocal damage model. *International Journal of Solids and Structures*, 46(6):1476–1490, 2009.

[9] C. Comi, S. Mariani, and U. Perego. An extended FE strategy for transition from continuum damage to mode I cohesive crack propagation. *International Journal for Numerical and Analytical Methods in Geomechanics*, 31(2):213–238, 2007.

[10] A. Simone, G. N. Wells, and L. J. Sluys. From continuous to discontinuous failure in a gradient-enhanced continuum damage model. *Computer Methods in Applied Mechanics and Engineering*, 192(41-42):4581–4607, 2003.

[11] M. Jirásek and T. Zimmermann. Embedded crack model: II. combination with smeared cracks. *International Journal for Numerical Methods in Engineering*, 50(6):1291–1305, 2001.

[12] G. N. Wells, L. J. Sluys, and R. De Borst. Simulating the propagation of displacement discontinuities in a regularized strain-softening medium. *International Journal for Numerical Methods in Engineering*, 53(5):1235–1256, 2002.

[13] A. Rodríguez-Ferran, I. Morata, and A. Huerta. A new damage model based on nonlocal displacements. *International Journal for Numerical and Analytical Methods in Geomechanics*, 29(5):473–493, 2005.

[14] N. Moës, J. Dolbow, and T. Belytschko. A finite element method for crack growth without remeshing. *International Journal for Numerical Methods in Engineering*, 46(1):131–150, 1999.

[15] T. Belytschko and T. Black. Elastic crack growth in finite elements with minimal remeshing. *International Journal for Numerical Methods in Engineering*, 45(5):601–620, 1999.

[16] A. Rodríguez-Ferran, T. Bennett, H. Askes, and E. Tamayo-Mas. A general framework for softening regularisation based on gradient elasticity. *International Journal of Solids and Structures*, 48(9):1382–1394, 2011.

[17] E. Tamayo-Mas and A. Rodríguez-Ferran. Condiciones de contorno en modelos de gradiente con desplazamientos suavizados. *Submitted*.